Cell Metabolism, Volume *34*

Supplemental information

Hypothalamic pregnenolone mediates recognition memory in the context of metabolic disorders

Sara Ramírez, Roberta Haddad-Tóvolli, Marija Radosevic, Miriam Toledo, Adriana Pané, Daniel Alcolea, Vicent Ribas, Maria Milà-Guasch, Macarena Pozo, Arnaud Obri, Elena Eyre, Alicia G. Gómez-Valadés, Iñigo Chivite, Tomas Van Eeckhout, Ioannis Zalachoras, Jordi Altirriba, Corinna Bauder, Mónica Imbernón, Gloria Garrabou, Carmen Garcia-Ruiz, Rubén Nogueiras, David Soto, Xavier Gasull, Carmen Sandi, Jens C. Brüning, Juan Fortea, Amanda Jiménez, José C. Fernández-Checa, and Marc Claret

Figure S1

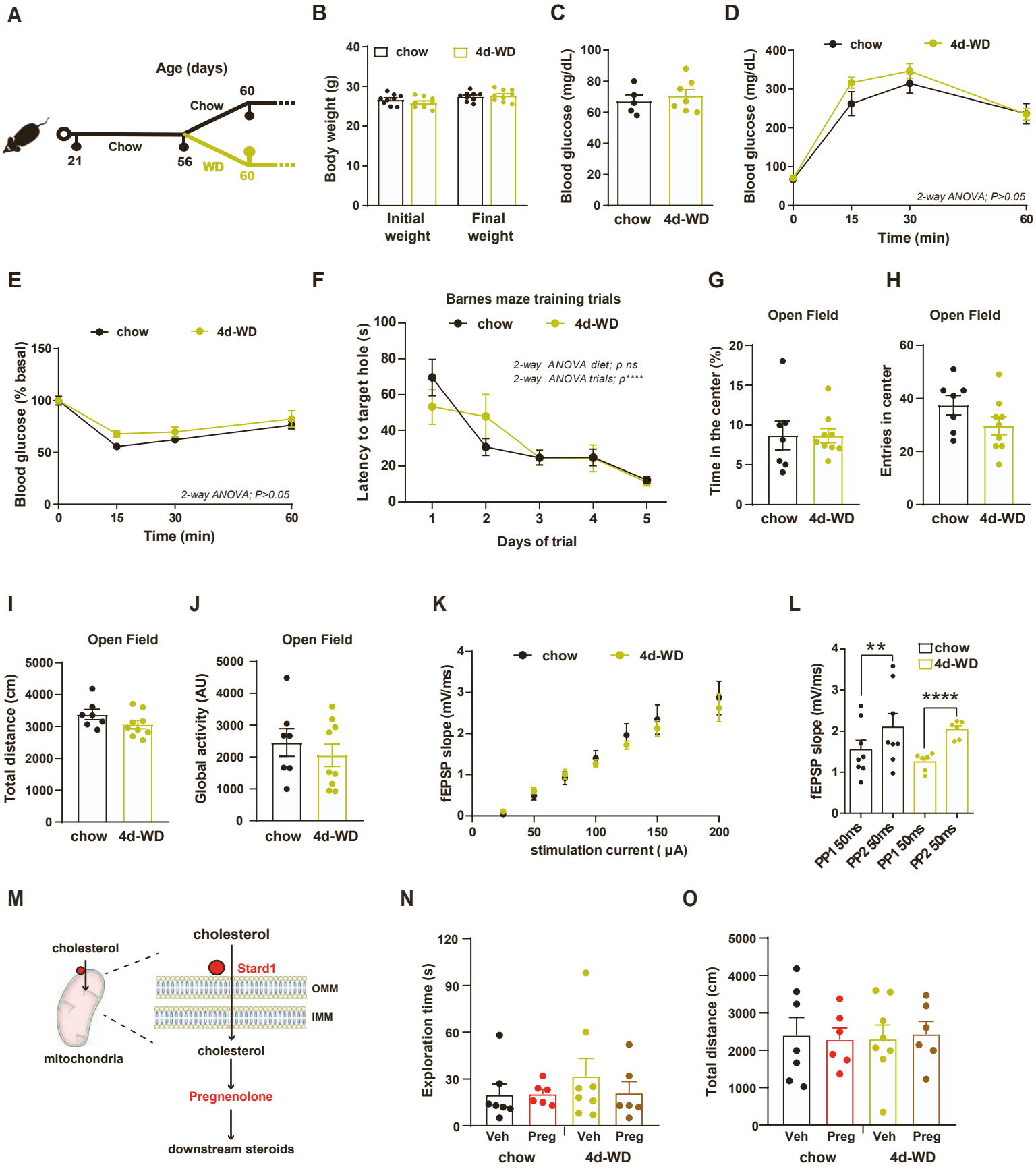
A
Age (days)
Chow
60
Chow
21
56
WD
60
B
chow
4d-WD
Body weight (g)
Initial weight
Final weight
C
Blood glucose (mg/dL)
chow
4d-WD
D
chow
4d-WD
Blood glucose (mg/dL)
2-way ANOVA; P>0.05
Time (min)
E
chow
4d-WD
Blood glucose (% basal)
2-way ANOVA; P>0.05
Time (min)
F
Barnes maze training trials
chow
4d-WD
2-way ANOVA diet; p ns
2-way ANOVA trials; p****
Latency to target hole (s)
Days of trial
G
Open Field
Time in the center (%)
chow
4d-WD
H
Open Field
Entries in center
chow
4d-WD
I
Open Field
Total distance (cm)
chow
4d-WD
J
Open Field
Global activity (AU)
chow
4d-WD
K
chow
4d-WD
fEPSP slope (mV/ms)
stimulation current (µA)
L
chow
4d-WD
**
****
fEPSP slope (mV/ms)
PP1 50ms
PP2 50ms
PP1 50ms
PP2 50ms
M
cholesterol
cholesterol
Stard1
OMM
IMM
mitochondria
cholesterol
Pregnenolone
downstream steroids
N
Exploration time (s)
Veh
Preg
Veh
Preg
chow
4d-WD
O
Total distance (cm)
Veh
Preg
Veh
Preg
chow
4d-WD

Figure S1. Short-term western-diet feeding impairs cognitive function in the absence of metabolic alterations (Related to Figure 1).

(A) Schematic illustration of the experimental strategy. C57Bl/6J mice at 56 days of age were submitted to either chow or western-diet for 4 consecutive days (4d-WD).

(B) Body weight at 56 days of age (initial weight) and after 4 days of western-diet (60 days of age; final weight) (n=9/diet).

(C) Basal blood glucose concentration in C57Bl/6J mice fed with either chow or western diet for 4 days (4d-WD) (n=5-7/diet).

(D) Glucose tolerance test in C57Bl/6J mice fed with either chow or western-diet for 4 days (4d-WD) (n=5-7/diet).

(E) Insulin sensitivity test in C57Bl/6J mice fed with either chow or western-diet for 4 days (4d-WD) (n=5-7/diet).

(F) Task learning curve for the latency to reach the scape hole during the training phase of the Barnes maze test (BMT) of chow and 4d-WD mice. Results show the average of 2 trials per day during 5 consecutive days (n=11/diet).

(G-J) Recorded parameters to assess open field performance in mice fed with either chow or 4d-WD: (G) time spent in the center; (H) number of entries in the center; (I) total distance travelled; (J) global activity (n=7-9/diet).

(K) Input/output characteristics of CA3-CA1 synapses in chow (n=7 recordings from 4 animals) and 4d-WD mice (n=7 recordings from 4 animals).

(**L**) Short-term plasticity at the Schaffer collateral - CA1 synapses showed paired-pulse facilitation (PPF) as measured by mean slope values of the fEPSPs in the response to the first (PP1) and second (PP2) stimulus. Both experimental groups showed a significant increase in the fEPSP slope upon second stimulus. Chow: n=7 recordings from 4 animals; 4d-WD: n=8 recordings from 4 animals. Interstimulus interval shown is 50 ms.

(M) Schematic illustration of pregnenolone biosynthesis, Stard1 location and function.

(N-O) Recorded parameters to assess NORT performance in C57Bl/6J mice fed with either chow or 4d-WD after central administration of vehicle or pregnenolone during the test phase: (N) exploration time (time exploring novel object + time exploring familiar object) and (O) total distance travelled (n=6-8/diet).

All studies were performed in male mice at 8-9 weeks of age. Dots in panels represent individual samples. Data are presented as mean ± SEM. **P<0.01; ****P<0.0001; ns: not significant.

Figure S2

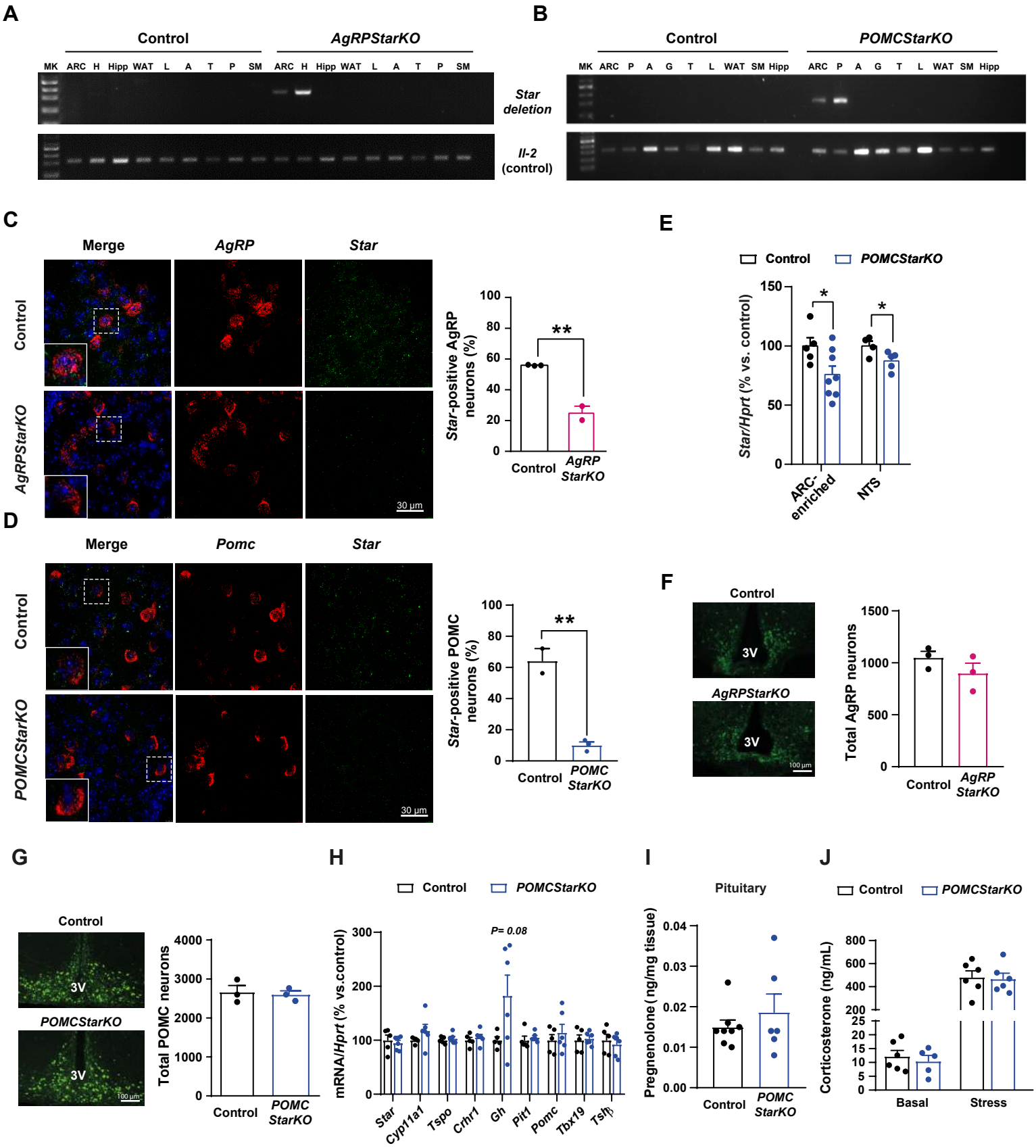
A
Control
AgRPStarKO
MK ARC H Hipp WAT L A T P SM ARC H Hipp WAT L A T P SM
Star deletion
Il-2 (control)
B
Control
POMCStarKO
MK ARC P A G T L WAT SM Hipp ARC P A G T L WAT SM Hipp
C
Merge
AgRP
Star
Control
AgRPStarKO
30 µm
Star-positive AgRP neurons (%)
Control
AgRP StarKO
D
Merge
Pomc
Star
POMCStarKO
Star-positive POMC neurons (%)
E
Control
POMCStarKO
Star/Hprt (% vs. control)
ARC-enriched
NTS
F
AgRPStarKO
3V
Total AgRP neurons
G
POMCStarKO
Total POMC neurons
H
P= 0.08
mRNA/Hprt (% vs.control)
Star
Cyp11a1
Tspo
Crhr1
Gh
Pit1
Pomc
Tbx19
Tshβ
I
Pituitary
Pregnenolone (ng/mg tissue)
J
Corticosterone (ng/mL)
Basal
Stress

Figure S2. Validation of mouse models with deletion of *Star* in AgRP or POMC neurons (Related to Figure 2).

(A-B) Detection of recombination of the floxed allele by PCR in diverse tissue samples from (A) *AgRPStarKO* and (B) *POMCStarKO* mice. A PCR reaction with interleukin 2 (Il-2) as internal control is also shown. MK: DNA size marker; ARC: arcuate-enriched hypothalamaus; H: mediobasal hypothalamus; Hipp: hippocampus; WAT: white adipose tissue; L: liver; A: adrenal gland; T: tail; P: pituitary; SM: skeletal muscle; G: gonad.

(C-D) Representative confocal images of fluorescent in situ hybridization colocalization of *Star* (green) with (C) *Agrp* (red) or (D) *Pomc* (red) in the arcuate nucleus of the hypothalamus from *AgRPStarKO* and *POMCStarKO* mice, respectively. Nuclear counterstaining was performed with DAPI (blue). Quantification is shown (n=2-3/genotype). Scale bar: 30 µm.

(E) *Star* expression analysis in the arcuate-enriched mediobasal hypothalamus and in the nucleus of the solitary tract (NTS) from control and *POMCStarKO* mice. *Hprt* was used as housekeeping gene (n=4-8/genotype).

(F-G) AgRP and POMC neuronal population size in the arcuate nucleus of the hypothalamus from (F) *AgRPStarKO* (n=3/genotype) and (G) *POMCStarKO* mice (n=3/genotype). Scale bar: 100 µm.

(H) Gene expression analysis in the pituitary from control and *POMCStarKO* mice. *Hprt* was used as housekeeping gene (n=5-6/genotype).

(I) Pregnenolone content in the pituitary from control and *POMCStarKO* mice (n=6-8/genotype).

(J) Basal and stressed corticosterone concentration in plasma from control and *POMCStarKO* mice (n=5-6/genotype).

All studies were performed in male mice between 10-16 weeks of age. Dots in panels represent individual samples. Data are presented as mean ± SEM. *P<0.05; **P<0.01.

Figure S3

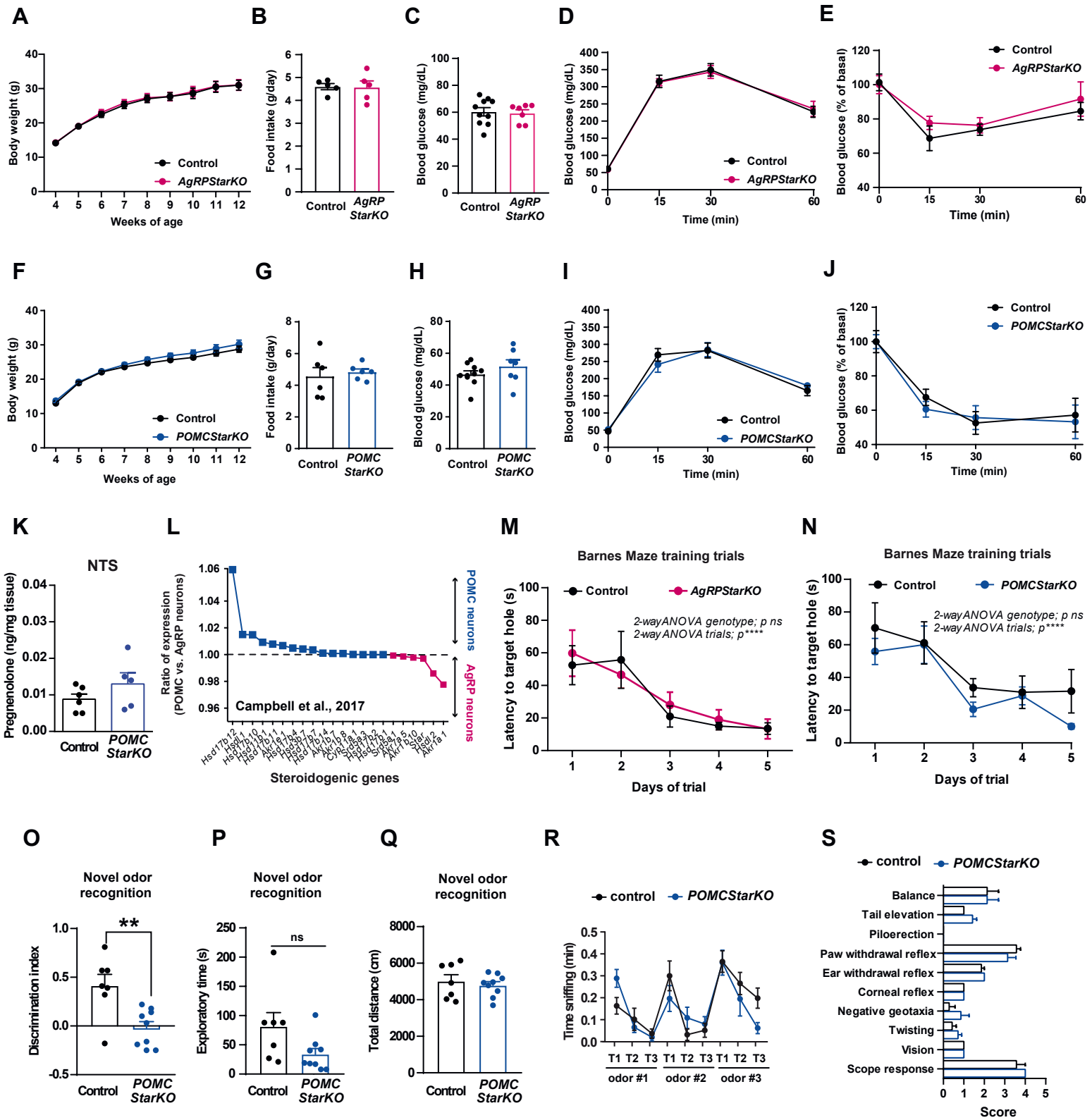
A
Body weight (g)
Weeks of age
Control
AgRPStarKO
B
Food intake (g/day)
Control
AgRP StarKO
C
Blood glucose (mg/dL)
Control
AgRP StarKO
D
Blood glucose (mg/dL)
Time (min)
Control
AgRPStarKO
E
Blood glucose (% of basal)
Time (min)
Control
AgRPStarKO
F
Body weight (g)
Weeks of age
Control
POMCStarKO
G
Food intake (g/day)
Control
POMC StarKO
H
Blood glucose (mg/dL)
Control
POMC StarKO
I
Blood glucose (mg/dL)
Time (min)
Control
POMCStarKO
J
Blood glucose (% of basal)
Time (min)
Control
POMCStarKO
K
NTS
Pregnenolone (ng/mg tissue)
Control
POMC StarKO
L
Ratio of expression (POMC vs. AgRP neurons)
Campbell et al., 2017
POMC neurons
AgRP neurons
Steroidogenic genes
M
Barnes Maze training trials
Latency to target hole (s)
Control
AgRPStarKO
2-wayANOVA genotype; p ns
2-wayANOVA trials; p****
Days of trial
N
Barnes Maze training trials
Latency to target hole (s)
Control
POMCStarKO
2-wayANOVA genotype; p ns
2-wayANOVA trials; p****
Days of trial
O
Novel odor recognition
Discrimination index
**
Control
POMC StarKO
P
Novel odor recognition
Exploratory time (s)
ns
Control
POMC StarKO
Q
Novel odor recognition
Total distance (cm)
Control
POMC StarKO
R
control
POMCStarKO
Time sniffing (min)
T1 T2 T3 T1 T2 T3 T1 T2 T3
odor #1
odor #2
odor #3
S
control
POMCStarKO
Balance
Tail elevation
Piloerection
Paw withdrawal reflex
Ear withdrawal reflex
Corneal reflex
Negative geotaxia
Twisting
Vision
Scope response
Score

Figure S3. Metabolic phenotyping of mouse models with deletion of *Star* in AgRP or POMC neurons (Related to Figure 2).

(A-E) Assessment of metabolic parameters in control and *AgRPStarKO* mice: (A) body weight profile (n=7-10/genotype); (B) daily food intake (n=5/genotype); (C) basal blood glucose (n=7-10/genotype); (D) glucose tolerance test (n=7-10/genotype); (E) insulin sensitivity test (n=7-10/genotype).

(F-J) Assessment of metabolic parameters in control and *POMCStarKO* mice: (F) body weight profile (n=18/genotype); (G) daily food intake (n=6/genotype); (H) basal blood glucose (n=7-10/genotype); (I) glucose tolerance test (n=7-10/genotype); (J) insulin sensitivity test (n=7-8/genotype).

(K) Pregnenolone content in the nucleus of the solitary tract (NTS) from control and *POMCStarKO* mice (n=6/genotype).

(L) Comparative analysis of the expression of neurosteroidogenic genes between AgRP and POMC neurons. Single-cell sequencing data was obtained from Campbell et al. 2017. Data is expressed as gene expression ratio.

(M-N) Task learning curve for the latency to reach the scape hole during the training phase of the Barnes maze test (BMT) in (M) *AgRPStarKO* (n=8/genotype) and (N) *POMCStarKO* mice (n=9-10/genotype). Results show the average of 2 trials per day during 5 consecutive days.

(O-Q) Recorded parameters to assess novel odor recognition test performance in *POMCStarKO* mice during the test phase: (O) discrimination index (time exploring novel object – time exploring familiar object) / (time exploring novel object + time exploring familiar object); (P) exploration time (time exploring novel object + time exploring familiar object); (Q) total distance travelled (n=7-9/genotype).

(R) Assessment of the smelling capacity of control and *POMCStarKO* mice to diverse social and non-social odors through trials (T1-T3) (n=6/genotype).

(S) Assessment of various neurosensory parameters in control and *POMCStarKO* mice (n=7/genotype).

All studies were performed in male mice between 10-16 weeks of age. Dots in panels represent individual samples. Data are presented as mean ± SEM. **P<0.01; ****P<0.0001; ns: not significant.

Figure S4

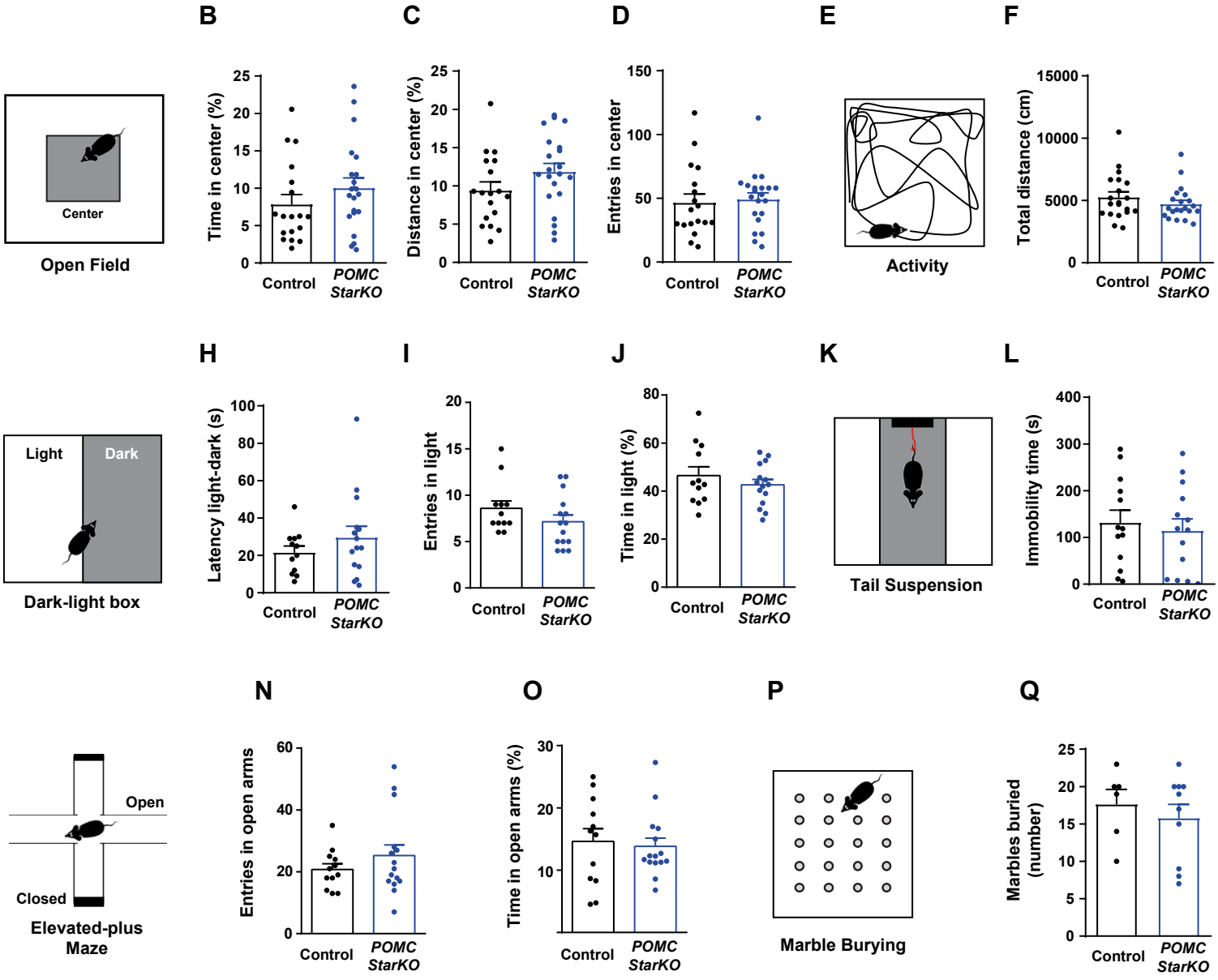
A
Center
Open Field
B
Time in center (%)
Control
POMC StarKO
C
Distance in center (%)
Control
POMC StarKO
D
Entries in center
Control
POMC StarKO
E
Activity
F
Total distance (cm)
Control
POMC StarKO
G
Light
Dark
Dark-light box
H
Latency light-dark (s)
Control
POMC StarKO
I
Entries in light
Control
POMC StarKO
J
Time in light (%)
Control
POMC StarKO
K
Tail Suspension
L
Immobility time (s)
Control
POMC StarKO
M
Open
Closed
Elevated-plus Maze
N
Entries in open arms
Control
POMC StarKO
O
Time in open arms (%)
Control
POMC StarKO
P
Marble Burying
Q
Marbles buried (number)
Control
POMC StarKO

Figure S4. Behavioral phenotyping of mice with deletion of *Star* in POMC neurons (Related to Figure 2).

(A) Schematic illustration of the open field task.

(B-D) Recorded parameters to assess open field performance in control and *POMCStarKO* mice: (B) time spent in the center; (C) distance travelled in the center; (D) number of entries in the center (n=18-21/genotype).

(E-F) Schematic illustration of the activity assessment task and (F) total distance travelled of control and *POMCStarKO* mice (n=20-21/genotype).

(G) Schematic illustration of the dark-light box task.

(H-J) Recorded parameters to assess performance during the dark-light box paradigm in control and *POMCStarKO* mice: (H) latency light-dark transition; (I) number of entries in illuminated zone; (J) time spent in the illuminated zone (n=12-15/genotype).

(K) Schematic illustration of the tail suspension test.

(L) Immobility time of control and *POMCStarKO* mice in a tail suspension test (n=13-14/genotype).

(M) Schematic illustration of the elevated-plus maze task.

(N-O) Recorded parameters to assess performance during the elevated-plus maze paradigm in control and *POMCStarKO* mice: (N) number of entries in open arms; (O) time spent in open arms (n=12-15/genotype).

(P) Schematic illustration of the marble burying test.

(Q) Number of marbles buried by control and *POMCStarKO* mice (n=6-10/genotype).

All studies were performed in male mice between 10-16 weeks of age. Dots in panels represent individual samples. Data are presented as mean ± SEM.

Figure S5

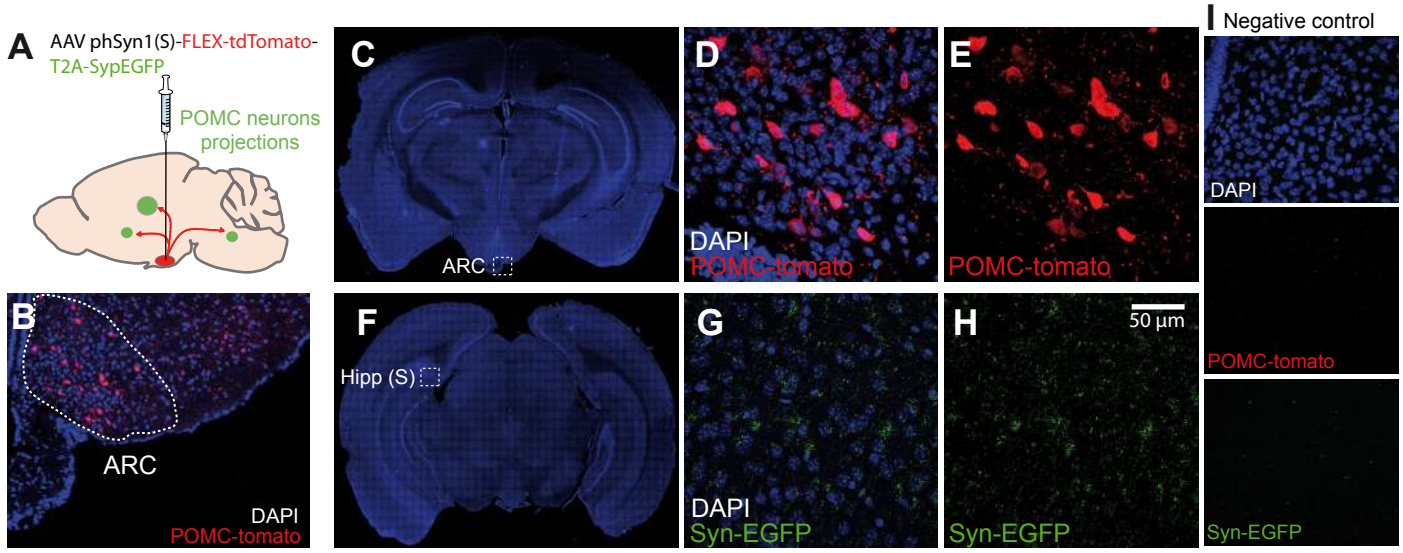
A
AAV phSyn1(S)-FLEX-tdTomato-T2A-SypEGFP
POMC neurons projections
B
ARC
DAPI
POMC-tomato
C
ARC
D
DAPI
POMC-tomato
E
POMC-tomato
F
Hipp (S)
G
DAPI
Syn-EGFP
H
50 µm
Syn-EGFP
Negative control
DAPI
POMC-tomato
Syn-EGFP

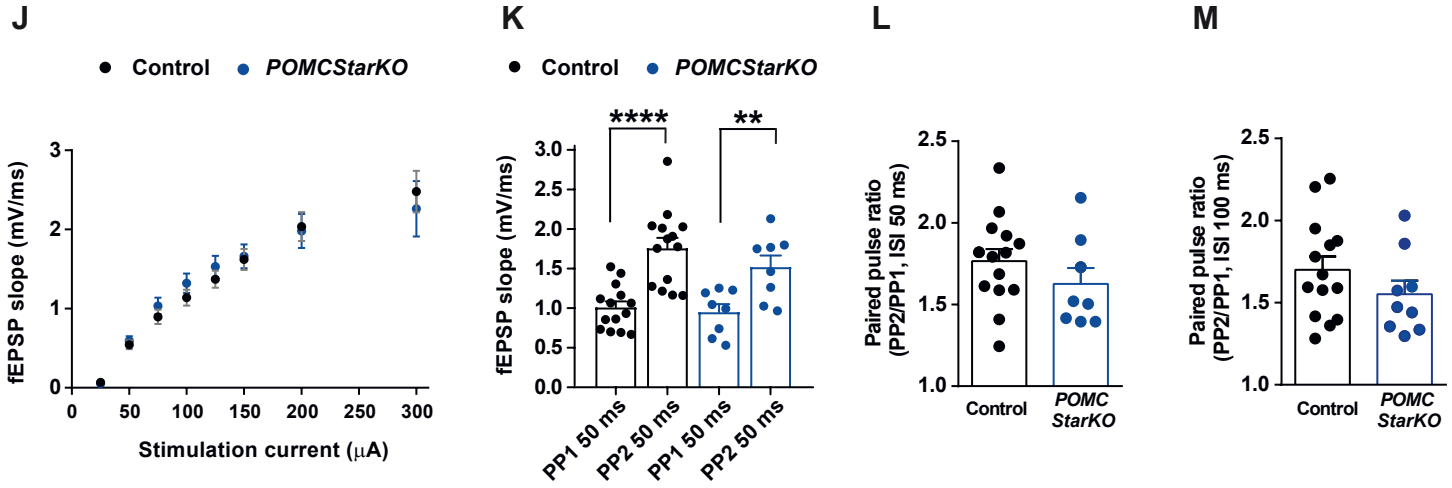
J
Control
POMCStarKO
fEPSP slope (mV/ms)
Stimulation current (µA)
K
Control
POMCStarKO
fEPSP slope (mV/ms)
****
**
PP1 50 ms
PP2 50 ms
PP1 50 ms
PP2 50 ms
L
Paired pulse ratio (PP2/PP1, ISI 50 ms)
Control
POMC StarKO
M
Paired pulse ratio (PP2/PP1, ISI 100 ms)
Control
POMC StarKO

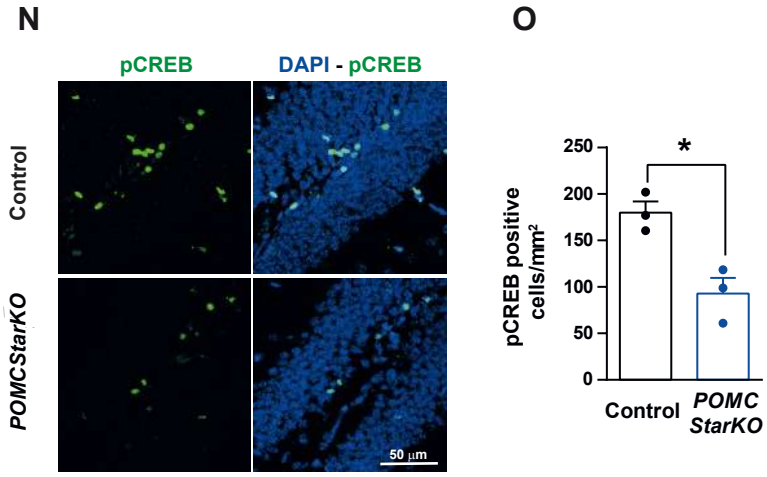
N
pCREB
DAPI - pCREB
Control
POMCStarKO
50 µm
O
pCREB positive cells/mm²
*
Control
POMC StarKO

Figure S5. Arcuate POMC neuron projections to hippocampal subiculum and long-term potentiation parameters (Related to Figure 2).

(A) Schematic depicting viral injection of *Cre*-dependent AAV-phSyn1(S)-FLEX-tdTomato-T2A-SypEGFP into the arcuate nucleus of the hypothalamus (ARC) of *POMC*$^{Cre/+}$ mice.

(B) Representative image of brain sections showing TdTomato expression (staining POMC neurons) in the ARC.

(C) Representative confocal images of a coronal section of the brain. Dotted inset depicts the ARC nucleus.

(D-E) TdTomato expression in the dotted area (ARC).

(F) Representative image of a coronal section of the brain. Dotted inset depicts the hippocampal subiculum area (Hipp (S)).

(G-H) EGFP expression (staining synaptophysin) in the hippocampal subiculum.

(I) Negative controls without primary antibody.

Scale bar: 50 µm.

(J) Input/output characteristics of CA3-CA1 synapses in control (n=14 recordings from 9 animals) and *POMCStarKO* mice (n=9 recordings from 5 animals).

(K) Short-term plasticity at the Schaffer collateral - CA1 synapses showed paired-pulse facilitation (PPF) as measured by mean slope values of the fEPSPs in the response to the first (PP1) and second (PP2) stimulus. Both experimental groups showed a significant increase in the fEPSP slope upon second stimulus. Controls: n=14 recordings from 9 animals; *POMCStarKO*: n=8 recordings from 5 animals. Interstimulus interval shown is 50 ms.

(L-M) Paired pulse facilitation, calculated as P2/P1 (pulse 2/pulse 1) fEPSP slope ratio, with interstimulus interval (ISI) of either 50 ms (L) or 100 ms (M).

(N) Representative confocal images of pCREB staining (green fluorescence) in the dentate gyrus of control and *POMCStarKO* mice under random-fed conditions. Scale bar: 50 µm.

(O) Quantification of pCREB positive cells (n=3/genotype).

All studies were performed in male mice between 10-16 weeks of age. Dots in panels represent individual samples. Data are presented as mean ± SEM. *P<0.05; **P<0.01; ****P<0.0001.

Figure S6

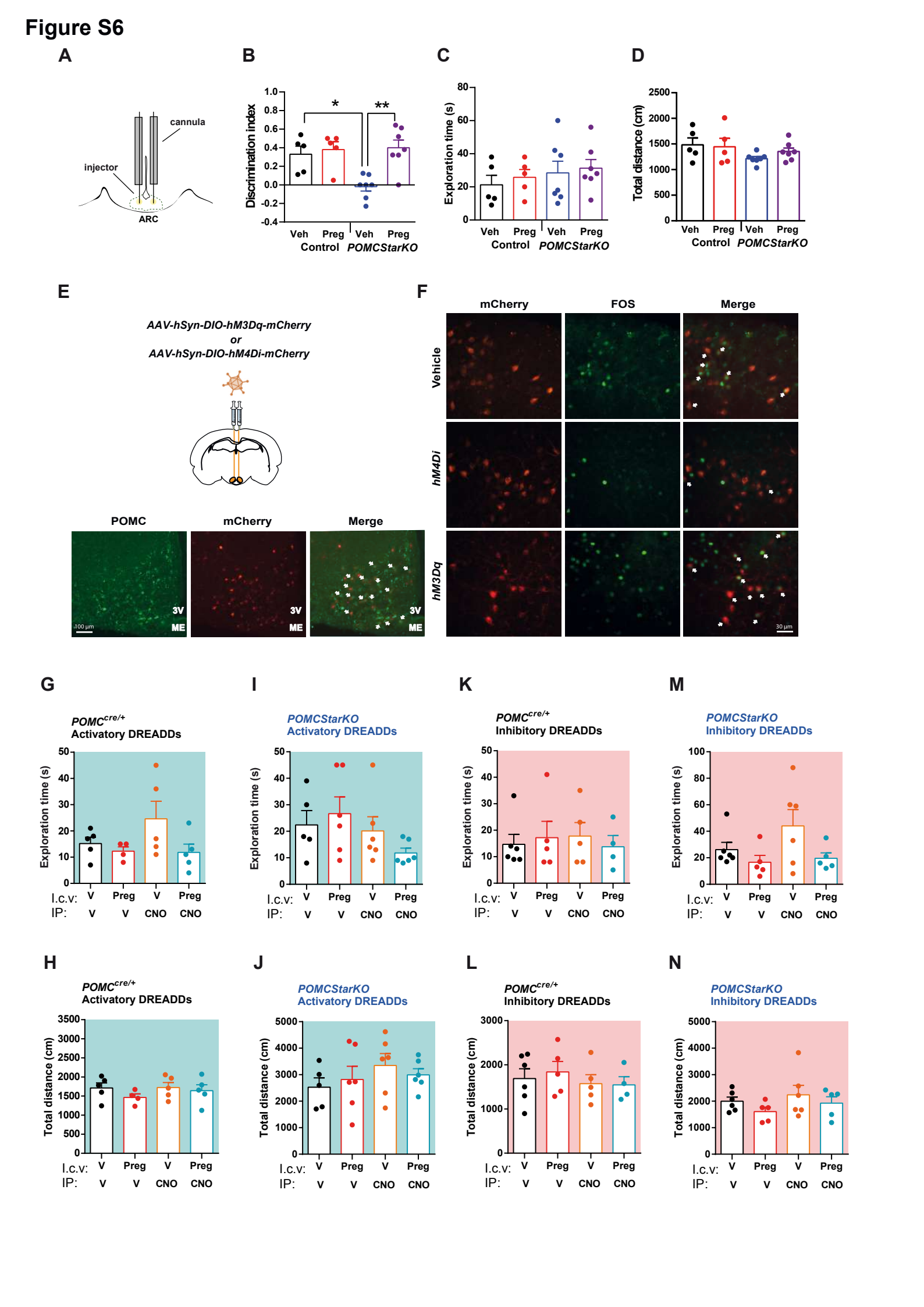
A
cannula
injector
ARC
B
Discrimination index
Veh
Preg
Veh
Preg
Control
POMCStarKO
C
Exploration time (s)
Control
POMCStarKO
D
Total distance (cm)
Control
POMCStarKO
E
AAV-hSyn-DIO-hM3Dq-mCherry
or
AAV-hSyn-DIO-hM4Di-mCherry
POMC
mCherry
Merge
3V
ME
100 µm
F
mCherry
FOS
Merge
Vehicle
hM4Di
hM3Dq
30 µm
G
POMCcre/+
Activatory DREADDs
Exploration time (s)
I.c.v:
IP:
V
Preg
CNO
I
POMCStarKO
Activatory DREADDs
K
POMCcre/+
Inhibitory DREADDs
M
POMCStarKO
Inhibitory DREADDs
H
POMCcre/+
Activatory DREADDs
Total distance (cm)
J
POMCStarKO
Activatory DREADDs
L
POMCcre/+
Inhibitory DREADDs
N
POMCStarKO
Inhibitory DREADDs

Figure S6. Validation of pregnenolone-arcuate effects and DREADD strategy (Related to Figure 4).

(A) Scheme illustrating bilateral cannulation into the arcuate nucleus of the hypothalamus (ARC).

(B-D) Recorded parameters to assess NORT performance in control and *POMCStarKO* mice, after central vehicle or pregnenolone administration, during the test phase: (B) discrimination index (time exploring novel object – time exploring familiar object) / (time exploring novel object + time exploring familiar object); (C) exploratory time (time exploring novel object + time exploring familiar object); (D) total distance travelled (n=5-7/genotype).

(E) Schematic illustration of the DREADD strategy used. Representative images of POMC and mCherry immunostaining of *POMC*$^{Cre/+}$ mice injected bilaterally, in the arcuate nucleus of the hypothalamus, with AAV-hSyn-DIO-hM3Dq-mCherry are shown. White arrows indicate colocalization. 3V: third ventricle; ME: median eminence. Scale bar: 100 µm.

(F) Representative images of FOS and mCherry immunostaining of *POMC*$^{Cre/+}$ mice, injected bilaterally in the arcuate nucleus of the hypothalamus, with AAV-hSyn-DIO-hM3Dq-mCherry or AAV-hSyn-DIO-hM4Di-mCherry. White arrows indicate colocalization. Scale bar: 30 µm.

(G-J) Recorded parameters to assess NORT performance in *POMC*$^{Cre/+}$ and *POMCStarKO* mice after POMC neuronal activation and central vehicle (V) or pregnenolone (Preg) administration during the test phase: (G) exploration time and (H) total distance travelled of *POMC*$^{cre/+}$ mice (n=4-5/genotype); (I) exploration time and (J) total distance travelled of *POMCStarKO* mice (n=5-6/genotype).

(K-N) Recorded parameters to assess NORT performance in *POMC*$^{Cre/+}$ and *POMCStarKO* mice after POMC neuronal inhibition and central vehicle (V) or pregnenolone (Preg) administration during the test phase: (K) exploration time and (L) total distance travelled of *POMC*$^{cre/+}$ mice (n=4-6/genotype); (M) exploration time and (N) total distance of *POMCStarKO* mice (n=5-6/genotype).

All studies were performed in male mice at 10 weeks of age. Dots in panels represent individual samples. Data is presented as mean ± SEM. *P<0.05; **P<0.001.

Table S1. Related to Figure 6. Anthropometric, clinical and cognitive features of the human cohort. MHO: Metabolically healthy obese (n=14); MUO: Metabolically unhealthy obese (n=26); M: male; F: female; BMI: body mass index; SBP: systolic blood pressure; DBP: diastolic blood pressure; HOMA-IR: homeostatic model assessment-insulin resistance; HbA1c: glycated hemoglobin; LDL: low-density lipoprotein; HDL: high-density lipoprotein; DM2: type-2 diabetes; MMSE: mini–mental state examination; CSF: cerebrospinal fluid. Data are shown as mean ± SEM.

Parameter	MHO patients	MUO patients	*P* value
N	14	26	-
M/F	7/7	11/15	-
Age (years)	49 ± 2	53 ± 1	0.11
BMI (Kg/m^2)	44 ± 1	43 ± 1	0.66
SBP (mmHg)	128 ± 3	131 ± 3	0.54
DBP (mmHg)	82 ± 3	81 ± 2	0.63
Fasting glycemia (mg/dL)	92 ± 2	117 ± 7	0.009
HOMA-IR	4 ± 1	10 ± 2	0.024
HbA1c (%)	5.4 ± 0.1	6.4 ± 0.2	0.0004
Triglycerides (mg/dL)	98 ± 10	149 ± 18	0.052
Cholesterol (mg/dL)	199 ± 9	182 ± 7	0.16
LDL (mg/dL)	120 ± 6	107 ± 5	0.13
HDL (mg/dL)	56 ± 3	46 ± 2	0.007
DM2 treatment (%)	0	69	-
Hypertension treatment (%)	0	69	-
Dyslipemia treatment (%)	0	31	-
MMSE score	29.3 ± 0.3	29.2 ± 0.1	0.74
Pregnenolone CSF (ng/ml)	0.60 ± 0.06	0.54 ± 0.05	0.51